ACCOUNTS
of chemical research

Core–Shell–Corona Polymeric Micelles as a Versatile Template for Synthesis of Inorganic Hollow Nanospheres

MANICKAM SASIDHARAN† AND KENICHI NAKASHIMA*

Department of Chemistry, Graduate School of Science and Engineering, Saga University, 1 Honjo-machi, Saga 840-8502, Japan

RECEIVED ON APRIL 9, 2013

CONSPECTUS

Hollow, inorganic nanoscale capsules have many applications, from the delivery of encapsulated products for cosmetic and medicinal purposes to use as lightweight composite materials. Early methods for producing inorganic hollow nanospheres using hard templates suffered from low product yield and shell weakness upon template removal. In the past decade, researchers have turned to amphiphilic copolymers to synthesize hollow nanostructures and ordered mesoporous materials.

Amphiphilic molecules self-assemble into well-defined nanostructures including spherical micelles. Micelles formed from simple, two-component AB diblock and ABA triblock copolymers, however, have been difficult to work with to construct inorganic hollow nanoparticles, because the corona of the micelle, which serves as the template for the shell, becomes unstable as it absorbs inorganic shell precursors, causing aggregates to form.

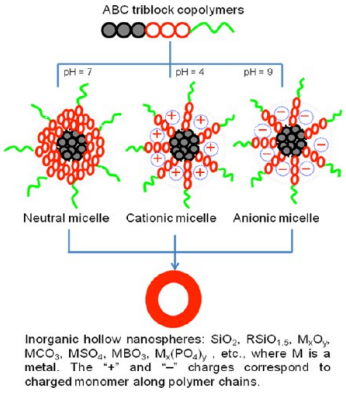

Newly developed, three-component ABC triblock copolymers may solve this problem. They provide nanoassemblies with more diverse morphological and functional features than AB diblock and ABA triblock copolymers. Micelles formed from ABC triblock copolymers in selective solvents that dissolve only one or two of the blocks provide templates for these improved nanoassemblies. By manipulating individual polymer blocks, one can "encode" additional features at the molecular level. For instance, modifying the functional groups or substitution patterns of the blocks allows better morphological and size control. Insights into polymer self-assembly gained over years of work in our group have set the stage to systematically engineer inorganic spherical hollow nanoparticles using ABC triblock copolymers.

In this Account, we report our recent progress in producing diverse, inorganic hollow spherical nanospheres from asymmetric triblock copolymeric micelles with core–shell–corona architecture as templates. We discuss three classes of polymeric micelles—with neutral, cationic, and anionic shell structures—that allow fabrication of a variety of hollow nanoparticles. Importantly, we synthesized all of these particles in water, avoiding use of hazardous organic solvents. We have designed the precursor of the inorganic material to be selectively sorbed into the shell domain, leaving the corona free from the inorganic precursors that would destabilize the micelle. The core, meanwhile, is the template for the formation of the hollow void. By rationally tailoring experimental parameters, we readily and selectively obtained a variety of hollow nanoparticles including silica, hybrid silicas, metal-oxides, metal-carbonates, metal-sulfates, metal-borates, and metal-phosphates.

Finally, we highlight the state-of-the-art techniques we used to characterize these nanoparticles, and describe experiments that demonstrate the potential of these hollow particles in drug delivery, and as anode and cathode materials for lithium-ion batteries.

1. Introduction

Synthesis of inorganic hollow nanostructures by soft-template approach remains a major challenge, and block copolymers could serve as versatile templates to obtain nanomaterials with well-defined shape and diverse chemical composition. Hollow capsules with nanometer-dimensions constitute an important class of materials that are employed in diverse technological applications, ranging from the delivery of encapsulated products for cosmetic and medicinal purposes to their use as lightweight composite materials.[1,2] The common strategy to generate inorganic hollow materials with controllable shapes is the application of templates, which act as a mold for the subsequent sol–gel reaction which can replicate the shape

Published on the Web 08/20/2013 www.pubs.acs.org/accounts
10.1021/ar4001026

of hard templates.[3,4] However, hard templates, which were extensively employed in the earlier production of inorganic hollow nanospheres, have several intrinsic disadvantages, such as low product yield due to the multistep synthetic process and lack of structural robustness of the shells upon template removal. In the past decade, amphiphilic copolymers have been used for synthesis of hollow nanostructures and ordered mesoporous materials.[5,6]

Despite the long history of amphiphiles,[7] they still continue to attract the attention of scientists, inspiring them to design new types of amphiphiles. The amphiphilic molecules, such as surfactants, can be made to self-assemble into micelles or vesicles with diverse structures when their concentration in solution exceeds some critical value called the critical micelle concentration (CMC).[8] Recently, the concept of amphiphiles has been extended to polymers that can self-assemble into micellar structures with defined sizes and shapes that may be used in applications such as soft templates for making nanostructured materials.[9−11] Compared with low-molecular-weight amphiphiles, polymeric counterparts have a structural diversity and stability. Amphiphilic block copolymers self-assemble into nanosized micelles after dissolution in a nonselective good solvent, followed by dialysis against water.[12] The self-assemblies fabricated using polymeric amphiphiles have a higher capacity for guest molecules, better thermal sustainability, and rich topologies which are widely anticipated to fabricate diverse functional nanomaterials.

The notable advantage of polymeric amphiphiles is that the size and morphology of the micelles can be easily tuned by adjusting the block size, polymer combination, and solvent composition. The polymeric micelles so far employed for the synthesis of inorganic materials have a *core–corona* type architecture formed either from AB diblock or ABA triblock copolymers.[13−16] In these systems, the corona of the micelles acts as a reservoir of the inorganic precursors, and the core acts as a template of the hollow. In this approach, however, the template micelles become very unstable when the precursor is sorbed into the corona, leading to the formation of aggregates. To circumvent these problems, we propose using ABC triblock copolymer micelles with a *core–shell–corona* structure as a soft template. In this Account, we intend to discuss and summarize our research efforts using different ABC triblock copolymers for the fabrication of diverse inorganic hollow nanospheres. As shown in Figure 1, we emphasize the synthesis of diverse inorganic hollow nanoparticles, such as silicas, hybrid silicas, metal oxide, metal carbonate, metal sulfate, metal phosphate, and metal borates

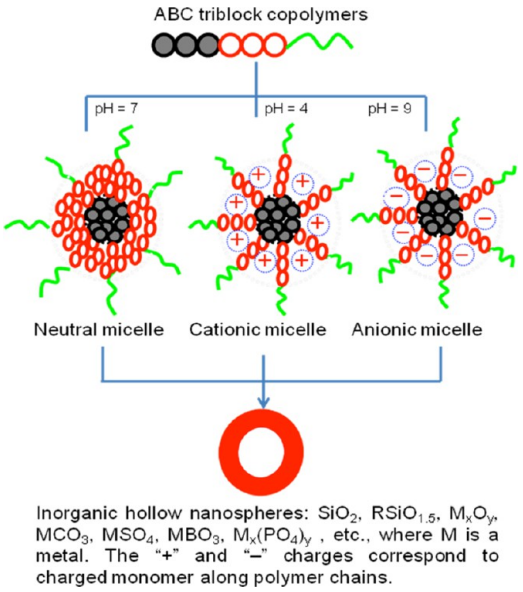

FIGURE 1. Polymeric micelles used for fabrication of inorganic hollow nanospheres.

using neutral, cationic, and anionic polymeric micelles with core–shell–corona structures in aqueous solutions. A comprehensive picture of the templating functions of soft micelles is highlighted, including micelle templating, formation pathway, properties, and salient applications, which we would expect to further promote the use of soft matter in inorganic nanoparticle fabrication.

2. Core–Shell–Corona Micelles for Inorganic Hollow Nanospheres

2.1. Neutral Micelles for Synthesis of Hollow Silica Nanospheres. The core–shell–corona (CSC) micelles with a PS core, a PVP shell, and a PEO corona of poly(styrene-*b*-2-vinylpyridine-*b*-ethylene oxide) (PS-PVP-PEO) is investigated for the fabrication of hollow silica nanospheres. The above micelle is neutral as such, but the shell domain of these micelles reversibly responds to a change in the environmental pH, due to the protonation of the PVP blocks, and this property has been successfully used to hydrolyze the silica precursors. It has been shown by Gohy et al. that the PS-PVP-PEO micelle has a glassy and hydrophobic PS-core, an ionizable hydrophilic PVP-shell, and a hydrophilic PEO-corona.[17,18] The PVP shell domain extends at low pH (<5) due to repulsive forces among the protonated PVP units. The addition of anionic species into this micelle cancels the positive charge of the PVP unit, resulting in a morphological change in the PVP shell from an extended to a shrunken form.[19] These behaviors of the CSC micelle have been utilized to selectively deposit the silica precursors on the

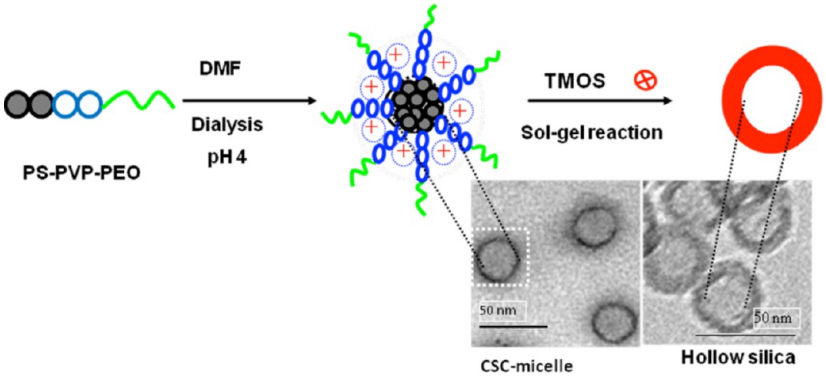

FIGURE 2. Formation of hollow silica nanospheres using PS-PVP-PEO micelles. Reproduced with permission from ref 20. Copyright 2007 American Chemical Society.

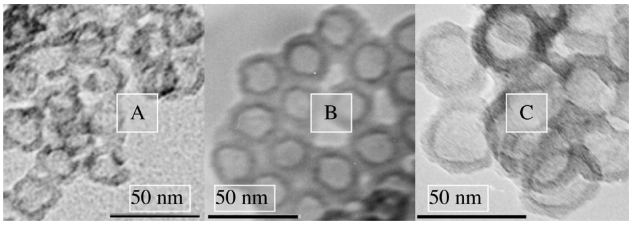

FIGURE 3. TEM images of hollow silica nanospheres. Template micelles: (A) [PS(14.1k)-PVP(12.3k)-PEO(8.5k)]; (B) [PS(20.1k)-PVP(14.2k)-PEO(26k)]; and (C) [PS(45k)-PVP(16k)-PEO(8.5k)]. Reproduced from refs 21 and 22 with permission. Copyright 2011 Royal Society of Chemistry and Copyright 2011 Elsevier Science.

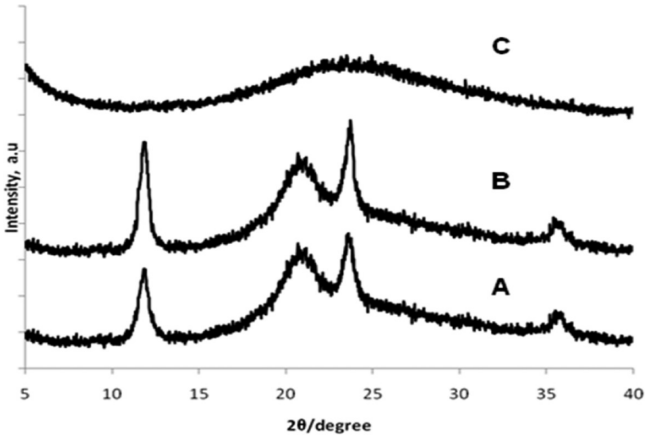

FIGURE 4. XRD of benzene-silica hollow nanospheres: (A) before calcinations; (B) after calcinations; and (C) calcined silica showing amorphous shell-domain. Reproduced from ref 24. Copyright 2011 Royal Society of Chemistry.

PVP block of the micelles for the following two reasons: (i) the protonated PVP block acts as an acid catalyst for the hydrolysis of tetramethoxysilane (TMOS), and (ii) hydrolyzed silica precursor species have a negative charge at pH 4 in order to strongly bind to the protonated PVP block. Thus, PS-core acts as a template for hollow void, PVP-shell domain serves as a reaction site for sol–gel reaction, and PEO-corona stabilizes the micelles. Figure 2 shows a typical procedure for fabricating hollow silica nanospheres with a template of the PS–PVP–PEO micelles using sol–gel techniques.[20]

The notable novelty of the CSC-micelle based strategy is that it allows us to tune the wall thickness and size of the void volume of the hollow silica nanospheres either by varying the TMOS/PVP molar ratios or controlling the PVP block length.[21] The size of the void volume of the hollow particles is controlled by the size of PS core. Figure 3 shows TEM images of hollow silica nanospheres synthesized with different polymers [PS(14.1k)-PVP(12.3k)-PEO(8.5k)], [PS(20.1k)-PVP(14.2k)-PEO(26k)], and [PS(45k)-PVP(16k)-PEO(8.5k)]. As the molecular weight of the PS block increased from 14k to 20k and then to 45k, the void space diameter of the hollow silica increased from 10 to 14 and then to about 20 nm.[21,22] Thus, the void space diameter can be fine-tuned on a scale of several nanometers by merely changing the PS block length, demonstrating the usefulness of the present method. However, the size of the PS-core (20 nm) is not strictly replicated in silica nanospheres (14 nm) due to shrinkage of the hollow particles during high temperature calcinations.[17]

2.2. Cationic Micelles for Hybrid Silica Hollow Nanospheres. As a significant development, the CSC micelles serve as efficient templates for the synthesis of organic/inorganic hybrid hollow particles. For instance, poly(styrene-[3-(methacryloylamino)propyl] trimethylammonium chloride-ethylene oxide) (PS-PMAPTAC-PEO) cationic micelles serve as templates from acidic to alkaline media.[23] The XRD pattern of hybrid benzene-silica hollow nanospheres (Figure 4A and B) prepared in an alkaline medium exhibited three additional diffraction peaks at high angles.[24] These results indicated the existence of a periodic structure or arrangement of the benzene groups (molecular-scale periodicity) with a spacing of 7.6 Å in the shell domain similar to periodic

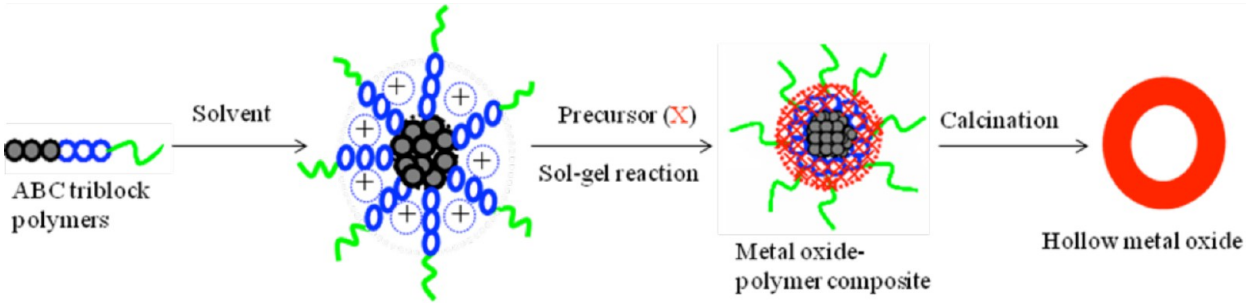

FIGURE 5. Formation of metal oxide hollow nanospheres over cationic micelles. Reproduced with permission from ref 26. Copyright 2009 American Chemical Society.

mesoporous benzene-silica.[25] The organization and assembly of hydrolyzed silica precursors at a microstructural level under basic conditions is different from acidic conditions,[25] and this property is indeed reflected in the fabrication benzene-silica hollow nanospheres under acidic (Figure 4C) and basic conditions (Figure 4A and B).

2.3. Cationic Micelles for Fabrication of Metal Oxide Hollow Nanospheres. To generalize the concept of cationic micelles, we have synthesized another cationic micelles by modifying the PS-PVP-PEO block copolymers by a quaternization reaction. The PVP block of the PS−PVP−PEO polymer was quaternized with iodomethane to obtain poly(styrene-*b*-2-vinyl-1-methylpyridinium iodide-*b*-ethylene oxide) (PS-PVMP-PEO). The resulting cationic micelles contain covalently quaternized PVMP units bearing permanent positive charge, which were used to fabricate Nb_2O_5, CeO_2, and V_2O_5 hollow spherical particles as shown in Figure 5.[26] The isoelectric points of respective metal precursors play a crucial role during the synthesis, and the isoelectric points of these metal oxides are around pH 4, 7, and 3, respectively, for Nb_2O_5, CeO_2, and V_2O_5. The metal oxide/polymer composite particles obtained by this process were calcined at 500 °C to obtain the metal oxide hollow nanospheres. The average particle size and void space diameter of the various metal oxide hollow nanospheres were 30 ± 2 and 18 ± 2 nm, respectively (Figure 6A−C). The estimated wall thickness was approximately 6 ± 1 nm. The high-resolution transmission electron microscope and XRD diffraction patterns of different metal oxides also confirmed their phase purity, and crystallinity.[27−29]

The previously described cationic PS-PMAPTAC-PEO micelles are highly efficient templates not only for silica but also for metal oxides such as MoO_3 and WO_3.[30,31] The self-assembly pathway involves an electrostatic interaction between the cationic PMAPTAC and the anionic MoO_4^{2-} and WO_4^{2-}. In a typical synthesis, appropriate amounts of $Na_2WO_4 \cdot 2H_2O$ or $Na_2MoO_4 \cdot 2H_2O$ were mixed with a polymeric micelle solution followed by acidification, aging, and calcinations. The XRD pattern of molybdenum oxide corresponds to β-MoO_3 with cell parameters $a = 7.12$, $b = 5.38$, $c = 5.55$, and $\beta = 91.9°$ (JCPDF 47-1081), and the WO_3 exhibited the characteristic orthorhombic lattice (PD-32-1394).[30,31] The TEM images of the WO_3 hollow nanospheres (Figure 6D) depict a uniform spherical hollow structure with a similar wall thickness. The average particle size was found to be 46 ± 2 nm with a cavity size of 14 ± 1 nm, and wall thickness of approximately 16 ± 1 nm. Similarly, the MoO_3 hollow particles (Figure 6E) exhibited a cavity diameter of approximately 16 ± 1 nm and a wall thickness of about 13 ± 1 nm (particle size was 42 ± 2 nm).

2.4. Anionic Micelles as Templates. The recently reported poly(styrene-*b*-acrylic acid-*b*-ethylene oxide) (PS-PAA-PEO) micelle was employed to demonstrate the efficacy of micelles with an anionic charge for the fabrication of inorganic hollow nanospheres.[32] The anionic micelles serve as efficient templates for reactive metal alkoxides, like Ti-alkoxides, Zr-alkoxides, Nb-alkoxides, and so forth. For example, in spite of the tremendous efforts by various research groups, it is difficult to synthesize titania (TiO_2) hollow nanospheres of few tens of nanometers in size mainly due to the lack of suitable soft templates and the complexity of the synthetic procedures involving extremely highly reactive titanium precursors. Figure 7 shows a schematic representation of the formation of titania hollow nanospheres.[33] In a basic medium, the PAA block containing −COOH ($pK_a = 4.6$) exists in the deprotonated form ($-COO^-$). Upon the addition of a catalytic amount of a dilute ammonia solution, the $-COO^-$ interacts with the positive NH_4^+ ions as evidenced from the change in the zeta potential from −57 to −29 mV for the micelles. The NH_4^+ ions play a crucial role in overcoming the repulsive barrier between the $-COO^-$ and negatively charged $\equiv TiO^-$ species (isoelectric point of titania ≈ 5). Upon the hydrolysis of tetrabutylorthotitanate (TBOT), the

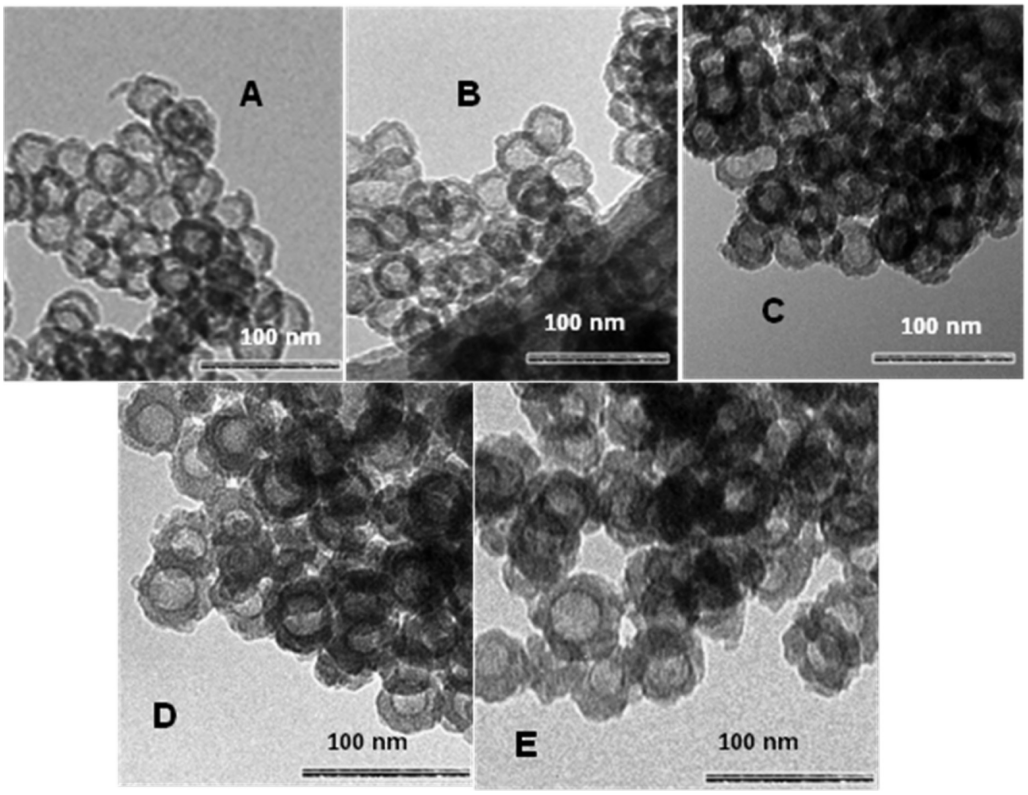

FIGURE 6. TEM pictures of (A) Nb_2O_5; (B) CeO_2; and (C) V_2O_5 hollow nanospheres templated by PS-PVMP-PEO micelles; (D) WO_3 and (E) MoO_3 hollow nanospheres templated by PS-PMAPTAC-PEO micelles. Reproduced from refs 27–29 and 30 with permission. Copyright 2012 Elsevier Science. Copyright 2012 Chemical Society of Japan. Copyright 2012 Electrochemical Society.

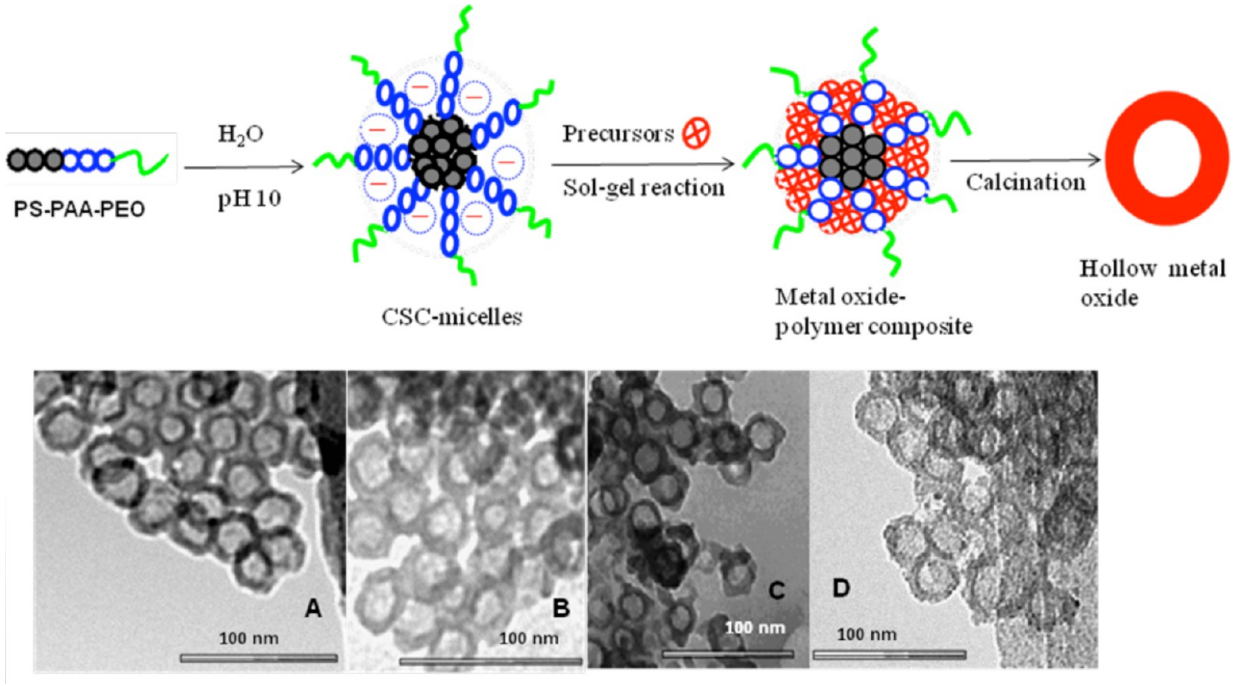

FIGURE 7. Schematic showing fabrication of hollow nanospheres with anionic CSC micelles: (A) TiO_2 (TBOT/PAA = 3); (B) TiO_2 (TBOT/PAA = 5); (C) La_2O_3; and (D) Fe_2O_3. Reproduced with permission from refs 33–35. Copyright 2011 and 2012, Royal Society of Chemistry. Copyright 2012 Elsevier Science.

resultant anionic ≡TiO$^-$ and their oligomers are adsorbed in the shell domain mediated by the NH_4^+ ions in a manner similar to the $S^-M^+I^-$ assembly mechanism. The composite particles were calcined to remove the polymeric templates as well as to crystallize the titania hollow shell structure. Figure 7A and B shows TEM images of the materials with TBOT/PAA mole ratios of "3" and "5". The average particle size and void space diameter were 28 ± 1 and 16 ± 1 nm, respectively. The wall thickness estimated by TEM was approximately 6 ± 1 nm. At lower TBOT/PAA ratios, the degree of aggregation of the nanospheres is quite low compared to the higher ratios. The XRD and high-resolution transmission electron microscopy (HRTEM) confirmed the purity and crystallinity of the titania hollow nanospheres.

Alternatively, the anionic CSC micelles can interact through an S^-I^+ mechanism in which the anionic $-COO^-$ ions bind with metal cations (M^+) and subsequently undergo sol−gel reactions. La_2O_3 and Fe_2O_3 hollow nanospheres were synthesized by the addition of $LaCl_3$ or $FeCl_3$ solutions to the above micelle.[34,35] The charge neutralization between the $-COO^-$ and M^{3+} ions was also evidenced from the change in the zeta potential from −55 to 0 mV with the gradual addition of M^{3+} ions to the micelle solution. Upon increasing the pH to about 10 using dilute NaOH, the clear micelle solution turns to gelatinous precipitates due to formation of metal hydroxides, which upon calcinations, lead to the formation of hollow nanospheres. This protocol also leads to nearly uniform hollow nanospheres with the average particle size of 30 ± 2 nm as shown in Figure 7C and D. As this method involves a simple electrostatic interaction of oppositely charged ions, it can be employed for the fabrication of a variety of metal oxide hollow nanospheres under mild conditions.

2.5. Metal-Carbonate and Metal-Sulfate Hollow Nanospheres. Calcium carbonate ($CaCO_3$) and barium sulfate ($BaSO_4$) are a scientifically and industrially important mineral system. Especially, the hollow structured calcium carbonates are quite useful as drug carriers because it has excellent biocompatible and biodegradable properties. These nanoparticles were synthesized using PS-PAA-PEO micelles with a core−shell−corona architecture.[36,37] Upon the addition of equimolar amounts of $CaCl_2$ and Na_2CO_3 to PS-PAA-PEO micelles under alkaline conditions (pH ≈ 10), $CaCO_3$ precipitates out in the PAA domain and forms composite particles. The composite particles were heated (500 °C) or solvent extracted with THF to obtain hollow particles. TEM pictures, Figure 8A and B, clearly confirm the formation of Ca^{2+}/PAA chelated particles and $CaCO_3$ hollow nanospheres,

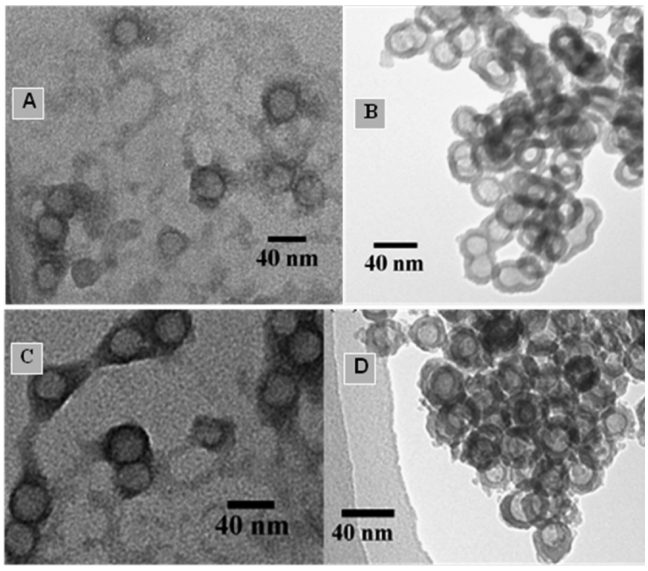

FIGURE 8. TEM images of: (A and C) PS-PAA-PEO micelles; (B and D) $CaCO_3$ and $BaSO_4$ hollow nanospheres. Reproduced from refs 36 and 37 with permission. Copyright 2011 American Chemical Society and Copyright 2012 Royal Society of Chemistry.

respectively. Similarly, $BaSO_4$ is formed through the electrostatic interaction between $-COO^-$ ions and Ba^{2+} ions and the formation of hollow spherical particles is confirmed by TEM images (Figure 8C and D).

2.6. Metal-Borate Hollow Nanospheres. The triblock copolymer micelles act as a smart soft template for the construction of hollow particles with a new chemical composition like lanthanum borate ($LaBO_3$) which is otherwise difficult to achieve by organizing inorganic precursors on a nanoscale level through a bottom-up approach.[38] Generally, $LaBO_3$ dense powders were synthesized by a high-temperature process (above 1000 °C); however, using PS-PAA-PEO micelles, $LaCl_3 \cdot 7H_2O$ and $NaBH_4$, $LaBO_3$ hollow nanospheres were synthesized under mild conditions. The La^{3+} ions readily precipitate as $La(OH)_3$ under alkaline conditions in the micelles' shell domain, which is the strongest base among the lanthanide metal ions due to its largest ionic radius (1.03 Å). On the other hand, after the decomposition of $NaBH_4$, the boron(III) reacts with hydroxide ions to form orthoboric acid. The formation of $La(OH)_3$ and $B(OH)_3$ is also clearly determined from the XRD.[38] The precursor-polymer composite particles were calcined at 600 °C to accomplish dehydration and extensive cross-linking in the three-dimensional network between $La(OH)_3$ and $B(OH)_3$.

Figure 9A−C shows TEM images of lanthanum borate synthesized with different La^{3+}/PAA ratios from 5 to 15 while maintaining the amount of boron constant. The TEM pictures of hollow particles show a uniform spherical shape,

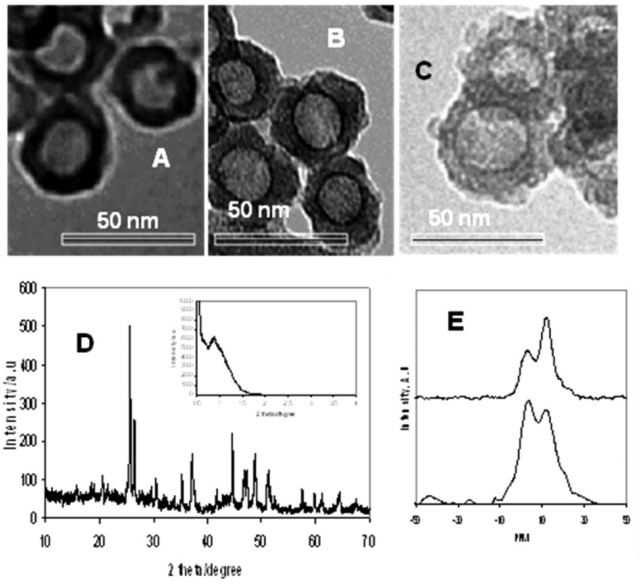

FIGURE 9. TEM images of $LaBO_3$ hollow nanospheres: (A) La^{3+}/PAA = 5; (B) La^{3+}/PAA = 10; (C) La^{3+}/PAA = 15; (D) wide-angle XRD (inset: SXRD); and (E) ^{11}B MAS NMR of sample (B). Reproduced from ref 38. Copyright 2011 Elsevier Science.

but the shell surface becomes rather rough at the high La^{3+} concentrations. At a lower La^{3+}/PAA ratio, the degree of aggregation of the nanospheres is quite low compared to that of the higher ratios. The average particle diameter increases with the La^{3+}/PAA ratio from 33 ± 2 to 36 ± 2 nm due to the adsorption of a large amount of the precursors in the shell domain. As the La^{3+}/PAA ratio increases from 5 to 15, the shell thickness also increased from 7 ± 2 to 10 ± 2 nm; however, the void space diameter remained nearly constant at 17 ± 2 nm. Figure 9D shows an XRD pattern of $LaBO_3$, which can be indexed as an orthorhombic structure with the lattice parameters of $a = 0.59$ nm, $b = 0.83$ nm, and $c = 0.51$ nm (JCPDS 12-0762). Quite interestingly, the SXRD pattern reveals the existence of disordered mesopores in the shell domain (Figure 9D, inset) which is consistent with the appearance of mesopores in the shell part of all the TEM pictures. The ^{11}B MAS NMR spectrum of $LaBO_3$ calcined at two different temperatures of 600 and 750 °C clearly confirms the presence of boron. The resonance peak at "0" ppm (Figure 9E) is attributed to tetrahedral sites, and the peak at 13 ppm is assigned to the trigonal borate species.

2.7. Metal-Phosphate Hollow Nanospheres. The anionic micelles serve as an ideal template for the synthesis of calcium phosphate (CaP) hollow nanospheres.[39] The fabrication of nanometer-sized hollow CaP spheres is rather difficult task due to the rapid precipitation and uncontrollable growth of the CaP crystals. However, the anionic micelle

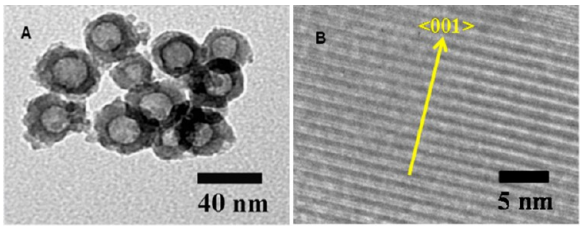

FIGURE 10. (A) Low-magnified and (B) high-magnified TEM images of CaP. Reproduced from ref 39. Copyright 2012 Royal Society of Chemistry.

PS-PAA-PEO under alkaline conditions overcomes this difficulty, through preferential coordination of the Ca^{2+} ions to the $-COO^-$ of the PAA blocks, leading to the formation of bidendate metal-polymer chelated particles. These chelated particles act as a soft template for the synthesis of calcium phosphate nanospheres. Mineralization of CaP takes place on the shell of the Ca^{2+}–PAA complex after addition of phosphate ions. The TEM image (Figure 10A) confirms the formation of uniform hollow spheres with an average particle size of about 30 nm. The HRTEM (Figure 10B) revealed that the (001) plane direction of the crystallized hydroxyapatite was well aligned. The wide-angle XRD patterns indeed confirmed the formation of the highly pure hydroxyapatite without any impurity phase.[39]

3. Application of Hollow Nanospheres

Inorganic hollow nanospheres possess important attributes like a low density, high surface-to-volume ratio, low thermal expansion coefficient, and low refractive index. These attributes make them attractive for applications including catalysis, antireflection surface coatings, rechargeable batteries, drug carriers, and sensors. In most cases, these characteristics make them superior to their bulk materials and they are thereby competitive in many important areas. We now provide a brief review of applications of hollow nanospheres in the areas of lithium ion batteries (LIB) and drug delivery studied by our research group.

3.1. Metal Oxide Hollow Nanospheres for Lithium Ion Batteries (LIB). Because of their advantages of high energy density, long life-cycle, no memory effect, and being environmentally benign, LIBs are currently the predominant power source for portable electronics and expected for use in electric vehicles in the near future. However, the use of metal oxides in LIBs is still largely hampered by their poor long-term cycling stability, energy density, and charge/discharge rate capability. We restrict our discussion to metal oxides evaluated in our laboratory and exclude reports pertaining to other nanostructures.[40] One effective way to

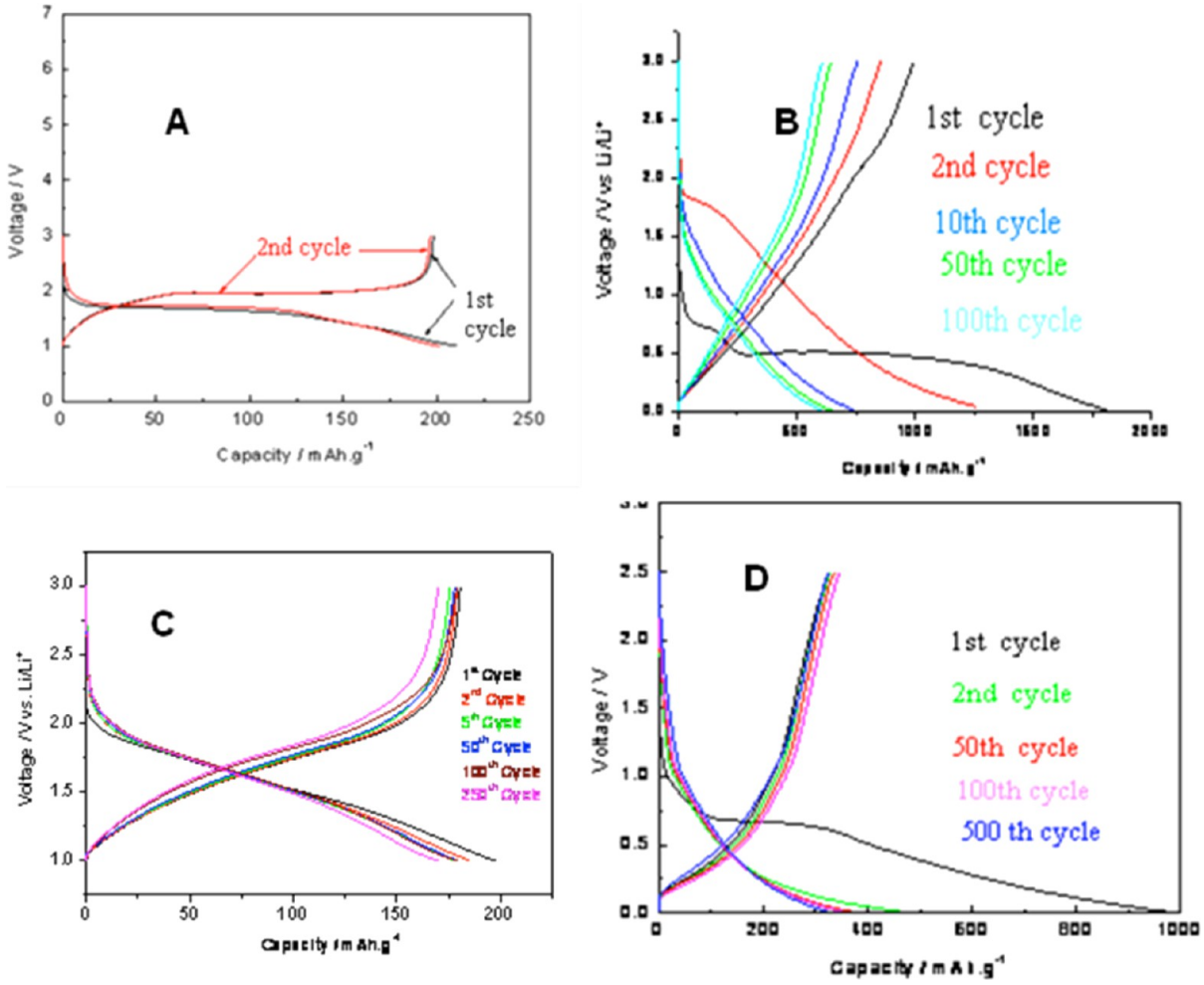

FIGURE 11. (A) Charge–discharge performance of TiO_2; (B) performance of hollow La_2O_3 nanospheres; (C) performance of Nb_2O_5 hollow nanospheres; and (D) electrochemical performance of hollow silica nanospheres. Reproduced from refs 21, 27, 33, and 34 with permission. Copyright 2011 and 2012 Royal Society of Chemistry. Copyright 2012 Elsevier Science.

mitigate these problems is to fabricate hollow structured active materials with high surface areas and short diffusion paths.[41] The thin shells of nanoparticles provide significantly reduced paths for both the insertion/extraction kinetics of Li^+ ions, giving rise to an improved cycling stability. As a result of significantly mitigated electrode pulverization and polarization, an exceptional electrochemical performance is thus highly anticipated for metal oxide hollow nanospheres. Figure 11 shows the electrochemical performance of representative metal oxide and silica (SiO_2) hollow nanospheres as anode materials for lithium ion batteries.

Figure 11A shows the discharge–charge profiles of TiO_2 for the first and second cycles at the 1 C rate (1.0–3.0 V versus Li/Li^+).[33] Interestingly, the first charge and discharge capacities are found to be 210.8 and 198.3 mAh g^{-1}, respectively, corresponding to a nominal insertion coefficient of $x = 0.6$, which exceeds the theoretical capacity of dense anatase TiO_2. The higher insertion coefficient may be attributed to the unique behavior of tiny hollow nanospheres with a thin shell having a high surface area which favors surface-confined charge storage. A remarkable feature of the TiO_2 hollow sphere is the very low irreversible capacity loss (6.3%) in the first cycle. To the best of our knowledge, none of the other reported TiO_2 particles showed this type of superior behavior. Additionally, the TiO_2 hollow particles demonstrated an excellent capacity retention over 50 cycles, and are able to deliver a reversible discharge capacity of 186.1 mAh g^{-1} higher than a previous report.[41,42] La_2O_3 hollow nanospheres, another interesting candidate, also exhibited a good electrochemical performance, such as long cycle life and very high columbic efficiency (Figure 11B).[34] The metallic lanthanum formed in the first reduction step alloys with lithium to form a Li_xLa alloy anode on the thin hollow shell domain. Generally, it is

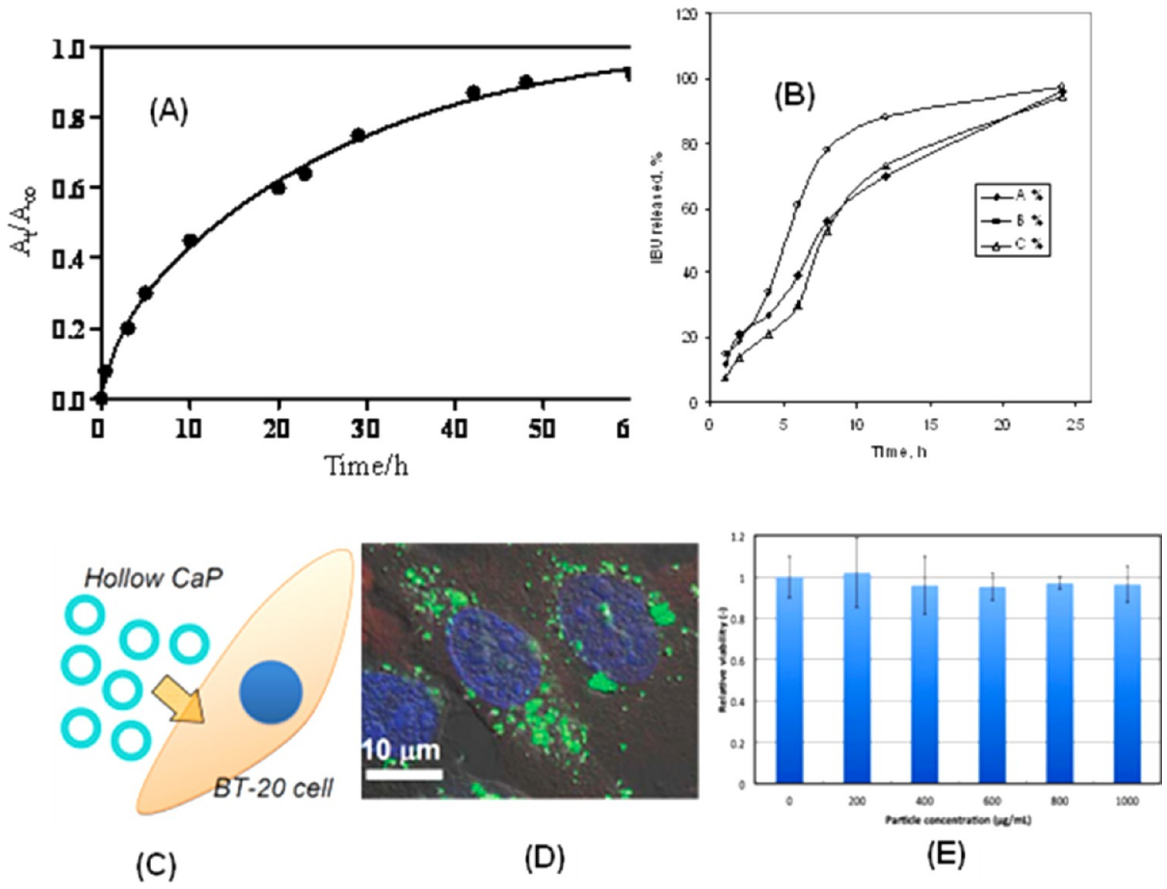

FIGURE 12. Drug-delivery profiles of (A) $CaCO_3$; (B) Fe_2O_3 and Fe_3O_4. (C) Schematic illustration of hollow CaP nanospheres for biocompatibility test;\. (D) A confocal fluorescent image of fluorescein-adsorbed hollow CaP nanoparticles (green dots) in BT-20 cancer cells. (E) MTT assays of BT-20 cells treated with hollow CaP nanoparticles of different concentrations. Reproduced from refs 35 and 36 with permission. Copyright 2012 Elsevier Science. Copyright 2011 American Chemical Society.

believed that alloying/dealloying leads to a significant capacity fading with cycling due to the volume change in the active electrode materials. However, the La_2O_3 hollow particles exhibit a high columbic efficiency and good cycleability even at high current densities which could be attributed to the existence of ultrasmall Li_xLa nanoparticles on the shell surface of the hollow nanosphere that provides a better electrical contact and shorter diffusion path length during repeated charge/discharge processes.

Similar to TiO_2, the Nb_2O_5 hollow nanosphere also showed stable electrochemical lithium intercalation/deintercalation reactions, and the nanoelectrode structure is highly stable with no deterioration of electrode observed even after 250 cycles of repeated charge/discharges (Figure 11C).[27] Another interesting candidate investigated in our laboratory for the first time is the use of hollow silica nanospheres as anode materials. It is generally expected that the reactivity of lithium with conventional bulk silica particles is quite low, but it tends to readily react with the silica nanoparticles. Figure 11D shows the charge/discharge capacity of Li^+ using a hollow silica nanosphere as the anode material. The discharge capacity values were found to be 980, 472, 355, 339, and 336 for the 1st, 2nd, 50th, 100th, and 500th cycles, respectively.[21] For the hollow silica particles, the Li^+ forms an isolated Li_2O/SiO_x nanomatrix in the silica shell wall. This is indeed reflected in the large difference in the capacities of the first cycle and subsequent cycles due to the formation of Li_2O. Furthermore, except for the first few cycles, the charge–discharge capacities of this hollow-silica based anode were maintained up to 500 cycles demonstrating a high columbic efficiency. Likewise, other metal oxide and metal borate hollow nanospheres, such as V_2O_5, CeO_2, MoO_3, Fe_2O_3, Fe_3O_4, and $LaBO_3$, also exhibit superior electrochemical properties as anode materials for lithium batteries.[28,29,31,38,43] The Fe_2O_3 and Fe_3O_4 hollow nanoparticles exhibit higher electrochemical performance than the nanotube and nanoflake based nanostructures.[43] The improved rate performance and discharge capacity of

these nanoconstructed electrodes is attributed partially to the unique hollow spherical morphology coupled with hollow void space. The void space not only acts as buffer medium against charge storage and local volume change but also provides better electrical contact and shorter diffusion path length and provides better rate capability.

3.2. Metal Oxide and Phosphate Hollow Nanoparticles as Drug Carrier Vehicles. There has been increased interest in inorganic nanoparticles as drug carriers. Among the many inorganic materials so far investigated for this purpose, $CaCO_3$ is highly suitable because of its excellent biocompatible and biodegradable properties. To investigate the release kinetics of naproxen from hollow $CaCO_3$ nanospheres,[36] the drug was loaded into $CaCO_3$ hollow nanospheres by suspending them in an aqueous solution, and the amount of drug loading/releasing was estimated by an in vitro method using UV−visible absorption spectrophotometry at 230 nm. The amount of the released naproxen was plotted versus time. Figure 12A shows the gradual and sustained release behavior of naproxen from $CaCO_3$ hollow particles over a period of 60 h. It is important to point out that the particle size significantly affects the cellular and tissue uptake, and only the nanosized particles can be efficiently internalized. In this regard, it is expected that the present hollow nanoparticle can be readily internalized into cells and tissue because the nanparticles' size (ca. 30 nm) is more ideal than the dense particle based carriers.

We have also investigated the efficacy of Fe_2O_3 and Fe_3O_4 hollow nanospheres as drug carriers after loading the ibuprofen (IBU) drug.[35] Figure 12B shows in vitro studies of the Fe_2O_3 and Fe_3O_4 hollow nanospheres as drug carriers using a phosphate buffer solution (PBS). Both magnetite and hematite show high storage capacities of 0.26−0.29 g per gram of hollow particles. The Fe_2O_3 exhibits a sustained release behavior over a period of 24 h at pH 7.3, and about 96% of the drugs were released into the solution after 24 h (curve A). For the Fe_3O_4 hollow nanospheres, the percentage of drug released at pH 7.3 is less than 55% after 8 h (curve C); whereas at pH 4, more than 80% of the ibuprofen was released over the same time period (curve B). These results demonstrated that the magnetic hollow nanospheres can be used as a sustainable and magnetically guided drug delivery carrier.

In addition to drug delivery, we have also investigated the biocompatibility with calcium phosphate hollow nanoparticles as biocompatibility is the prime factor in medical applications. The safety and toxicological issues of the hollow calcium phosphate (CaP) nanospheres were examined by MTT assays of a breast cancerous cell line (BT-20) incubated with various concentrations of hollow CaP nanospheres.[39] The results shown in Figure 12C and D indicate that the cell viability was as high as the control sample, even when the CaP concentration was up to 1000 μg/mL, demonstrating an excellent biocompatibility in vitro.

4. Conclusions and Outlook

The study of the molecular self-assembly of amphiphilic polymers has witnessed a paradigm shift from the mere serendipitous observations of soft micelle nanostructures to the meticulous formation of well-defined inorganic hard materials. This study relates recent developments in the creation of diversified micelle templates for different inorganic hollow nanosphere fabrication, characterization, and applications. Core−shell−corona micelles have provided various means to synthesize hollow spherical particles with different chemical compositions. However, success in this templating strategy hinges largely on the stability of the polymeric micelles, and therefore, factors that influence the behavior of amphiphilic molecules should be carefully considered. Compared with conventional AB diblock and ABA triblock copolymer micelles, the use of ABC triblock copolymer micelles with a core−shell−corona architecture overcomes the instability of polymeric micelles during hard-material fabrication. Though *core−shell−corona* micelles enable the facile formation of spherical hollow particles, a lot more needs to be unraveled so far as the basics of self-assembly with inorganic precursors and their structural transformation into other interesting nanostructures. One of the most important challenges is to prevent agglomeration of the hollow nanoparticles due to their inherent high surface energy, which is very important for applications in electronics, photonic devices, and drug delivery. In this regard, one can improve the dispersion of nanoparticles by ultrasonication in the absence of any stabilizing agents. In particular, the precise control of the size, shape, and morphologies and understanding the self-assembly processes should further be developed in order to obtain their new or enhanced properties and applications.

We thank the Japanese Society for Promotion of Science (JSPS) for their research support (Grant No. 20310054).

BIOGRAPHICAL INFORMATION

Manickam Sasidharan, currently working as a Professor in the SRM Research Institute, obtained his Ph.D. in chemistry in 1996 from the National Chemical Laboratory (CSIR, India). His postdoctoral

work focused on material synthesis, characterization, and applications in the areas of sustainable green catalysis, sensors, lithium-ion batteries, capacitors, and solar cells.

Kenichi Nakashima received his Ph.D. in physical chemistry from Kyushu University in 1985. He has been a professor at Saga University since 1987. He worked with Professor Mitchell A. Winnik at the University of Toronto as a visiting assistant professor for one year. During his stay at the University of Toronto, he studied polymer latexes, polymer blends, and polymeric micelles. Current research projects in his laboratory focus on inorganic hollow nanoparticles, stimuli-responsive polymeric micelles, and photoreactions in polymer nanosystems.

FOOTNOTES

*To whom correspondence should be addressed. E-mail: nakashik@cc.saga-u.ac.jp.
The authors declare no competing financial interest.
The manuscript was written through contributions of all the authors. All authors have approved the final version of the manuscript.
†Present address: SRM Research Institute, SRM University, Kattankulathur, Chennai-602203, India.

REFERENCES

1 Martin, C. R.; Kohli, P. The emerging field of nanotube biotechnology. *Nat. Rev. Drug Discovery* **2003**, *2*, 29–37.

2 Xu, Z. P.; Zeng, Q. H.; Lu, G. Q.; Yu, A. B. Inorganic nanoparticles as carriers for efficient cellular delivery. *Chem. Eng. Sci.* **2006**, *61*, 1027–1040.

3 Caruso, F. Hollow capsule processing through colloidal templating and self-assembly. *Chem.—Eur. J.* **2000**, *6*, 413–419.

4 Caruso, F. Nanoengineering of particle surfaces. *Adv. Mater.* **2001**, *13*, 11–22.

5 Deng, Y.; Wei, J.; Sun, Z.; Zhao, D. Large-pore ordered mesoporous materials template from non-pluronic amphiphilic block copolymers. *Chem. Soc. Rev.* **2013**, *42*, 4054–4070.

6 Niu, D.; Ma, Z.; Li, Y.; Shi, J. Synthesis of core-shell structured duel-mesoporous silica spheres with tunable pore size and controllable shell thickness. *J. Am. Chem. Soc.* **2010**, *132*, 15144–15147.

7 Israelachvili, J. N.; Mitchell, D. J.; Ninham, B. W. Theory of self-assembly of hydrocarbon amphiphiles into micelles and bilayers. *J. Chem. Soc., Faraday Trans. 2* **1976**, *72*, 1525–1568.

8 Ringdorf, H.; Schlarb, B.; Venzmer, J. Molcular architecture and function of polymeric oriented systems: Models for the study of organization, surface recognition, and dynamics of biomembranes. *Angew. Chem., Int. Ed.* **1988**, *27*, 113–158.

9 Moffitt, M.; Khougaz, L.; Eisenberg, A. Micellization of ionic block copolymers. *Acc. Chem. Res.* **1996**, *29*, 95–102.

10 Alexandridis, P. Amphiphilic copolymers and their applications. *Curr. Opin. Collid Interface Sci.* **1996**, *1*, 490–501.

11 Chen, D. Y.; Jiang, M. Strategies for constructing polymeric micelles and hollow spheres in solution via specific intermolecular interactions. *Acc. Chem. Res.* **2005**, *38*, 494–502.

12 Willet, N.; Gohy, J. F.; Auvray, L.; Varshney, S.; Jerome, R.; Leyh, B. Core–shell–corona micelles by PS-b-MP-b-PEO copolymers: Focus on the water-induced micellization process. *Langmuir* **2008**, *24*, 3009–3015.

13 Bergbreiter, D. E. Self-assembled sub-micrometer diameter semipermeable capsules. *Angew. Chem., Int. Ed.* **1999**, *38*, 2870–2872.

14 Lee, H.; Char, K. Morphological changes from silica tubules to hollow silica spheres controlled by the intermolecular interactions within block copolymer micelle templates. *ACS Appl. Mater. Interfaces* **2009**, *1*, 913–920.

15 Caruso, F.; Caruso, R. A.; Mohwald, H. Nanoengineering of inorganic and hybrid hollow spheres by colloidal templating. *Science* **1998**, *282*, 1111–1114.

16 Kramer, E.; forster, S.; Goltner, C.; Antonietti, M. Synthesis of nanoporous silica with new pore morphologies by templating the assemblies of ionic block copolymers. *Langmuir* **1998**, *14*, 2027–2031.

17 Gohy, J. F.; Willet, N.; Varshney, S.; Zhang, J. X.; Jerome, R. Core–shell–corona micelles with a responsive shell. *Angew. Chem., Int. Ed.* **2001**, *40*, 3214–3216.

18 Lei, L.; Gohy, J. F.; Willet, N.; Zhang, J. X.; Varshney, S.; Jerome, R. Tuning the morphology of core–shell–corona micelles in water: Transition from sphere to cylinder. *Macromolecules* **2004**, *37*, 1089–1094.

19 Khanal, A.; Li, Y.; Takisawa, N.; Kawasaki, N.; Oishi, Y.; Nakashima, K. Morphological change of the micelle of poly(styrene)-b-poly(2-vinylpyridine)-b-poly(ethylene oxide) induced by binding of sodium dodecylsufate. *Langmuir* **2004**, *20*, 4809–4812.

20 Khanal, A.; Inoue, Y.; Yada, M.; Nakashima, K. Synthesis of silica hollow nanoparticles template by polymeric micelle with core–shell–corona structure. *J. Am. Chem. Soc.* **2007**, *129*, 1534–1535.

21 Sasidharan, M.; Liu, D.; Gunawardhana, N.; Yoshio, M.; Nakashima, K. Synthesis, characterization and application for lithium-ion rechargeable batteries of hollow silica nanospheres. *J. Mater. Chem.* **2011**, *21*, 13881–13888.

22 Liu, D.; Sasidharan, M.; Nakashima, K. Micellles of poly(styrene-b-2-vinylpyridine-b-ethylene oxide) with blended polystyrene core and their application to the synthesis of hollow silica nanospheres. *J. Colloid Interface Sci.* **2011**, *358*, 354–359.

23 Liu, J.; Liu, D.; Yokoyama, Y.; Yusa, S.; Nakashima, K. Physichemical properties of micelles of poly(styrene-b-[3-(methacryloylamino)propyl] trimethylammonium chloride-b-poly-(ethylene oxide) in aqueous solution. *Langmuir* **2009**, *25*, 739–743.

24 Sasidharan, M.; Nakashima, K.; Gunawardhana, N.; Yokoi, T.; Ito, M.; Inoue, M.; Yusa, S.; Yoshio, M.; Tatsumi, T. Periodic organosilica hollow nanospheres as anode materials for lithium ion rechargeable batteries. *Nanoscale* **2011**, *3*, 4768–4773.

25 Inagaki, S.; Guan, S.; Ohsuna, T.; Terasaki, O. An ordered mesoporous organosilica hybrid material with a crystal-like wall structure. *Nature* **2002**, *416*, 304–307.

26 Liu, D.; Nakashima, K. Synthesis of hollow metal oxide nanospheres by templating polymeric micelles with core–shell–corona architecture. *Inorg. Chem.* **2009**, *48*, 3898–3900.

27 Sasidharan, M.; Gunawardhana, N.; Yoshio, M.; Nakashima, K. Nb_2O_5 hollow nanospheres as anode material for enhanced performance in lithium ion batteries. *Mater. Res. Bull.* **2012**, *47*, 2161–2164.

28 Sasidharan, M.; Gunawardhana, N.; Yoshio, M.; Nakashima, K. CeO_2 hollow nanospheres as anode material for lithium ion batteries. *Chem. Lett.* **2012**, *41*, 386–388.

29 Sasidharan, M.; Gunawardhana, N.; Yoshio, M. Nakashima, V_2O_5 hollow nanospheres: A lithium intercalation host with good rate capability and capacity retention. *J. Electrochem. Soc.* **2012**, *159*, A618–A621.

30 Liu, J.; Sasidharan, M.; Liu, D.; Yokoyama, Y.; Yusa, S.; Nakashima, K. Novel MoO_3 and WO_3 hollow nanospheres assembled with polymeric micelles. *Mater. Lett.* **2012**, *66*, 25–28.

31 Sasidharan, M.; Gunawardhana, N.; Noma, H.; Yoshio, M.; Nakashima, K. α-MoO_3 hollow nanospheres as an anode material for Li-ion batteries. *Bull. Chem. Soc. Jpn.* **2012**, *85*, 642–646.

32 Yusa, S.; Yokoyama, Y.; Morishima, Y. Synthesis of oppositely charge block copolymers of poly(ethylene glycol) via reversible addition-fragmentation chain transfer radical polymerization and characterization of their polyion complex micelles in water. *Macromolecules* **2009**, *42*, 376–383.

33 Sasidharan, M.; Nakashima, K.; Gunawardhana, N.; Yokoi, T.; Inoue, M.; Yusa, S.; Yoshio, M.; Tatsumi, T. Novel titania hollow nanospheres of size 28 ± 1 nm using soft-templates and their application for lithium-ion rechargeable batteries. *Chem. Commun.* **2011**, *47*, 6921–6923.

34 Sasidharan, M.; Gunawardhana, N.; Inoue, M.; Yusa, S.; Yoshio, K.; Nakashima, K. Novel La_2O_3 hollow nanospheres as high performance anode materials for Li-ion rechargeable batteries. *Chem. Commun.* **2012**, *48*, 3200–3203.

35 Sasidharan, M.; Luitel, H. N.; Gunawardhana, N.; Inoue, M.; Yusa, S.; Watari, T.; Nakashima, K. Synthesis of magnetic α-Fe_2O_3 and Fe_3O_4 hollow nanospheres for sustained release of ibuprofen. *Mater. Lett.* **2012**, *73*, 4–7.

36 Bastakoti, B. P.; Guragain, S.; Yokoyama, Y.; Yusa, S.; Nakashima, K. Synthesis of Hollow $CaCO_3$ nanospheres template by micelles of poly(styrene-b-acrylic acid-b-ethylene glycol) in aqueous solutions. *Langmuir* **2011**, *27*, 379–384.

37 Bastakoti, B. P.; Guragain, S.; Yokoyama, Y.; Yusa, S.; Nakashima, K. Synthesis of hollow $BaSO_4$ nanospheres template by core–shell–corona type polymeric micelles. *New J. Chem.* **2012**, *36*, 125–129.

38 Sasidharan, M.; Gunawardhana, N.; Luitel, H. N.; Yokoi, T.; Inoue, M.; Yusa, S.; Watari, T.; Yoshio, M.; Tatsumi, T.; Nkashima, K. Novel $LaBO_3$ hollow nanospheres of size 34 ± 2 nm template by polymeric micelles. *J. Colloid Interface Sci.* **2011**, *370*, 51–57.

39 Bastakoti, B. P.; Inoue, M.; Yusa, S.; Liao, S.; Wu, K. C. W.; Nakashima, K.; Yamauchi, Y. A block copolymer micelle template for synthesis of hollow calcium phosphate nanospheres with excellent biocompatibility. *Chem. Commun.* **2012**, *48*, 6532–6534.

40 Lou, X. W.; Archer, A. L.; Yang, Z. Hollow micro-/nanostructures: synthesis and applications. *Adv. Mater.* **2008**, *20*, 3987–4019.

41 Wang, Z.; Zhou, L.; Lou, X. W. Metal oxide hollow nanostructures for lithium-ion batteries. *Adv. Mater.* **2012**, *24*, 1903–1911.

42 Wu, H. B.; Chen, J. S.; Hng, H. H.; Lou, X. W. Nanostructured metal oxide-based materials as advanced anodes for lithium-ion batteries. *Nanoscale* **2012**, *4*, 2526–2542.

43 Sasidharan, M.; Gunawardhan, N.; Yoshio, M.; Nakashima, K. α-Fe_2O_3 and Fe_3O_4 hollow nanospheres as high-capacity anode materials for rechargeable Li-ion batteries. *Ionics* **2013**, *19*, 25–31.